| | | |
|---|---|---|
| | COMP | down |
| | ANK3 | down |
| | EPB41L3 | up |
| | ALX1 | down |
| | PDLIM3 | up |
| | SHOX2 | down |
| | HOPX | up |
| | EPB41L3 | up |
| | B4GALT1 | down |
| | COL12A1 | down |
| | DNER | up |
| | HOXD10 | up |
| | FRMD5 | up |
| | COL12A1 | down |

表 4. 骨芽細胞の機能別遺伝子発現

| Function | Gene | Regulation (Patient to Normal) |
|---|---|---|
| Hedgehog | HHIP | up |
| Inflammation | COL3A1 | up |
| | COL1A1 | up |
| | AGT | up |
| | APOE | up |
| | F2R | up |
| | IL6 | down |
| | AGTR1 | up |
| | C5 | up |
| | TNFAIP6 | down |
| | TAC1 | down |
| | SCN9A | up |
| | CXCL3 | down |
| | CD24 | up |
| | FOS | down |
| | CXCL2 | down |
| | COL3A1 | up |
| | CCL2 | down |
| | SCN9A | up |
| | COL3A1 | up |
| Osteoblast | IL6 | down |
| | NOG | down |
| Surface Receptor | STC2 | down |
| | C5 | up |
| | OXTR | up |
| | CD24 | up |
| | TNFRSF10B | down |
| | GPR126 | up |
| | CCL2 | down |
| Cell adhesion | CD9 | up |
| | NRCAM | down |
| | NID2 | up |
| | COL11A1 | up |
| | FLRT2 | down |
| | HAPLN1 | up |
| | PCDH7 | up |
| | ACAN | up |
| | COMP | down |
| | TNFAIP6 | down |
| | HAS1 | down |
| | ACAN | up |
| | COL21A1 | up |

| | | |
|---|---|---|
| Skeletal | MYH11 | up |
| | KRT19 | up |
| | COL1A1 | up |
| | COL1A2 | up |
| | DMD | down |
| | VDR | down |
| | COL11A1 | up |
| | CLEC3B | up |
| | ACAN | up |
| | COMP | down |
| | MEOX2 | up |
| | EPB41L3 | up |
| | ALX1 | down |
| | HOPX | up |
| | EPB41L3 | up |
| | SDC2 | up |
| | EPB41L3 | up |
| | HOXD10 | up |
| | TBX15 | down |
| | NOG | down |

# III. 研究成果の刊行に関する一覧表

研究成果の刊行に関する一覧表

書籍

| 発表者氏名 | | 書籍名 | 出版会社 | ページ | 出版年 |
|---|---|---|---|---|---|
| 竹谷健 | 低フォスファターゼ症 | 先天性代謝異常ハンドブック | 中山書店 | 412-413 | 2013 |

雑誌

| 発表者氏名 | 論文タイトル名 | 発表誌名 | 巻号 | ページ | 出版年 |
|---|---|---|---|---|---|
| Ohnishi H, Oda Y, Aoki T, Tadokoro M, Katsube Y, Ohgushi H, Hattori H, Yuba S | A comparative study of induced pluripotent stem cells generated from frozen, stocked bone marrow- and adipose tissue-derived mesenchymal stem cells | JTissue Eng Regen Med | 6 | 261-267 | 2012 |
| Shimizu Y, Kihara T, Haghparast SM, Yuba S, Miyake J | Simple display system of mechanical properties of cells and their dispersion | PLoS One | 7 | e34305 | 2012 |
| Tadokoro M, Matsushima A, Kotobuki N, Hirose M, Kimura Y, Tabata Y, Hattori K, Ohgushi H | Bone morphogenetic protein-2 in biodegradable gelatin and β-tricalcium phosphate sponges enhances the in vivo bone-forming capability of bone marrow mesenchymal stem cells | J Tissue Eng Regen Med | 6 | 253-260 | 2012 |
| Ogawa M, Tohma Y, Ohgushi H, Takakura Y, Tanaka Y. | Early Fixation of Cobalt-Chromium Based Alloy Surgical Implants to Bone Using a Tissue-engineering Approach | Inn J Mol Sci | 13 | 5528-5541 | 2012 |

# Ⅳ. 研究成果の刊行物・別刷

# 低フォスファターゼ症


## SUMMARY

低フォスファターゼ症は，組織非特異的アルカリフォスファターゼ（*TNSALP*）遺伝子変異によりALP活性が低下して骨の石灰化障害をきたす疾患である．

骨の石灰化に必要なヒドロキシアパタイト結晶は，カルシウムと無機リン酸などから形成される．その構成成分である無機リンは，ALPがピロリン酸を加水分解することにより産生される．また，ピロリン酸は無機リンに拮抗してヒドロキシアパタイト結晶の形成を阻害する．すなわち，本疾患はALP活性が低下していることにより，ピロリン酸から無機リンへの合成が阻害され，ピロリン酸が蓄積するためにヒドロキシアパタイト結晶の形成が障害され，骨の石灰化が起こらなくなる（**図1**）．

臨床症状は発症時期により重症度が異なっており，一般的に周産期に発症した場合は致死的な経過をとり，生後6か月以降に発症する場合は生命予後は良好であるが，低身長や乳歯の早期脱落などをきたす．血清ALPの低値で診断され，ほとんどの症例が常染色体劣性遺伝形式をとり，遺伝子型と表現型との間に関連がある．確立した治療法はないが，酵素補充療法や間葉系幹細胞移植などの臨床研究が進んでいる．


## 代謝障害と病態

骨の石灰化は，骨芽細胞と軟骨細胞由来の基質小胞で始まる．この基質小胞の中に含まれるカルシウムと無機リン酸が最初に形成されるヒドロキシアパタイト結晶の構成成分である．この結晶が細胞外に放出されて，コラーゲンやオステオカルシン，オステオポンチン，オステオネクチンなどのタンパク質とリン酸カルシウムが結合して骨が形成される．しかし，細胞外に存在するピロリン酸は無機リンに拮抗してヒドロキシアパタイトの結晶形成を阻害する（**図1**）．すなわち，正常の石灰化には無機リンとピロリン酸のバランスが保たれていることが必要である．

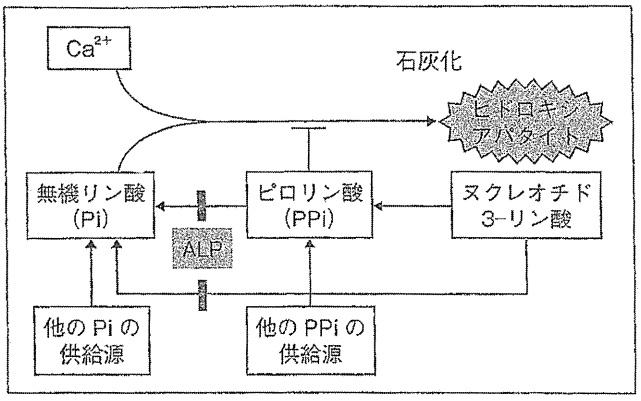


**図1　石灰化の機序**

この無機リンとピロリン酸を調節する因子として，ALP，plasma cell membrane glycoprotein-1（PC-1），ankylosis（ANK），osteopontin（OPN）などがある．ALPは基質小胞や骨芽細胞膜に存在してピロリン酸を加水分解して無機リンを増加させる．PC-1は基質小胞や骨芽細胞膜に存在してヌクレオチド3-リン酸からピロリン酸を産生する．ANKは，骨芽細胞膜に存在してピロリン酸を細胞内から細胞外に運び出す無機リン酸トランスポーターである．OPNはヒドロキシアパタイト結晶の形成を阻害する．このように，ALPは石灰化を促進し，PC-1，ANK，OPNは石灰化を抑制する．

## 臨床病型

低フォスファターゼ症は，多くは常染色体劣性遺伝形式をとるが，致死的でない軽症の場合，常染色体優性の遺伝形式を示す例もある．その障害部位は，主に骨と歯に症状が限定されている．

臨床症状は，胎内で死亡する重症から，成人してから発症するタイプまで，発症時期や重症度がさまざまである．同胞間でも異なった臨床像を示すことがあるが，発症年齢と臨床症状に基づいて，6つの臨床型に分類される（**表1**）．

表1　低フォスファターゼ症の臨床病型

| 臨床型 | 遺伝形式 | 臨床像 | 歯の特徴 |
|---|---|---|---|
| 1. 周産期型（致死型） | AR | 呼吸障害，けいれん，石灰化障害 | − |
| 2. 周産期型（良性） | AD | 長幹骨の変形，骨折<br>出生後石灰化が改善 | ± |
| 3. 乳児型 | AR | 体重増加不良，高カルシウム血症，石灰化障害，くる病様変化 | 早期脱落（乳歯） |
| 4. 小児型 | AD<br>AR | 低身長，歩行障害，骨痛，骨折，骨幹端から骨幹に向かう舌状突出 | 早期脱落（乳歯） |
| 5. 成人型 | AD<br>AR | ストレス骨折（中足骨），偽骨折（大腿骨），軟骨石灰化症 | ± |
| 6. 歯限局型 | AD<br>AR | 早期脱落（乳歯），う歯，歯槽骨喪失，歯髄腔の拡大 | 左に同じ |

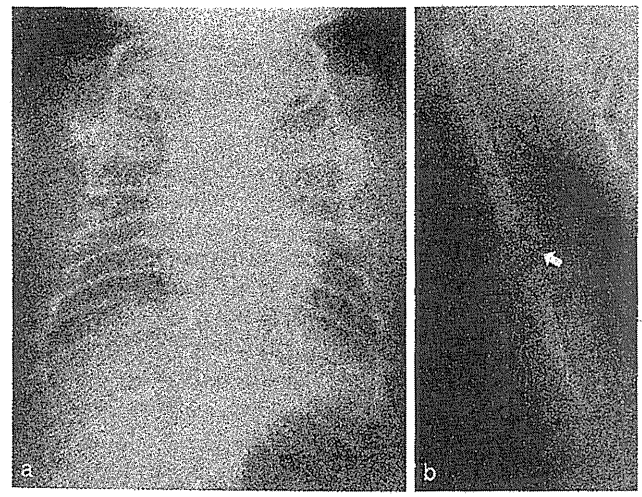


**図2　低フォスファターゼ症のX線写真**
a：胸部．狭胸郭，肋骨の菲薄化．b：上腕骨．矢印は，骨幹端から骨幹に向かうX線透過性の舌状突出を示す．

## 診断

**①生化学検査**：血清ALPの低下は全例で認められる．臨床症状の重症度と血中ALP値には相関がみられる．乳児型では高Ca血症と高Ca尿症のみられることが多い．小児型と成人型において，無機リンはしばしば高値を示す．また，ALPの基質であるホスホエタノールアミンは高値を示す．これは，血中・尿中アミノ酸分析で調べることができるが，いくつかの骨代謝疾患でも上昇する．

**②X線検査**：臨床病型により骨・歯のX線所見は異なるが，石灰化障害，長幹骨の変形，骨幹端の不整，狭胸郭，骨幹端から骨幹に向うX線透過性の舌状突出，骨幹端の拡張，肋軟骨の念珠形成などが認められる（**図2**）．

**③遺伝子検査**：ほとんどの患者（95%以上）で*TNSALP*遺伝子変異が見つかっている．遺伝子変異の集中している領域はなく，翻訳領域全領域にわたって変異が認められ，79%がミスセンス変異であり，常染色体劣性遺伝形式をとる重症型はホモ接合体よりも複合ヘテロ接合体の頻度が高い．TNSALP変異タンパクのALP残存活性と臨床的重症度が相関する．日本人では，c1559delTとpPhe327Leuの2つの変異が多く認められるが，前者は周産期型（致死型）と相関が高いのに対して，後者は周産期に発症するにもかかわらず致死的ではない．

## 治療

現在，これまで確立した根治療法はなく，対症療法が中心となる．しかし，最近，ALPを効率的に骨に到達させるために，アミノ酸を付加した酵素補充療法や骨芽細胞・軟骨に分化する間葉系幹細胞の移植治療の臨床研究が行われており，根治療法として期待されている．

## 予後

予後は病型によって異なる．周産期・乳児期に呼吸障害を認める例は致死的な経過をとるが，周産期発症でも呼吸障害がない場合は，生命予後は良好である．しかし，予後良好な乳児型や小児型も，乳歯が早期に脱落したり，低身長を合併するため，QOLは必ずしも良くない例が多い．

●文献

1) Whyte MP. Ann N Y Acad Sci 2010；1192：190-200.
2) Mornet E. Best Pract Res Clin Rheumatol 2008；22：113-27.
3) 竹谷健ほか．小児科 2009；50増刊：1169-76.
4) Whyte MP, et al. N Engl J Med 2012；366：904-13.
5) Tadokoro M, et al. J Pediatr 2009；154：924-30.

（竹谷　健）

JOURNAL OF TISSUE ENGINEERING AND REGENERATIVE MEDICINE
*J Tissue Eng Regen Med* 2012;**6**: 261–271.
Published online 27 June 2011 in Wiley Online Library (wileyonlinelibrary.com) **DOI:** 10.1002/term.428

RESEARCH ARTICLE

# A comparative study of induced pluripotent stem cells generated from frozen, stocked bone marrow- and adipose tissue-derived mesenchymal stem cells

Hiroe Ohnishi[1], Yasuaki Oda[1], Tetsuhiro Aoki[1,2], Mika Tadokoro[1], Yoshihiro Katsube[1]
Hajime Ohgushi[1], Koji Hattori[1] and Shunsuke Yuba[1]*
[1]*Tissue Engineering Research Group, Health Research Institute, National Institute of Advanced Industrial Science and Technology (AIST), Amagasaki site, Amagasaki, Hyogo, Japan*
[2]*Shinshu University, Department of Orthopaedic Surgery, Asahi, Matsumoto, Nagano, Japan*

## Abstract

**Bone marrow-derived mesenchymal stem cells (BMSCs) and adipose tissue-derived mesenchymal stem cells (AMSCs) have been used clinically for tissue regeneration; however, their proliferation/differentiation potentials are limited. Recently, induced pluripotent stem cells (iPSCs), known to have nearly unlimited potential to proliferate and differentiate into cells of all three germ layers, have gained wide interest in regenerative medicine. Here, we generated iPSCs from frozen-stocked AMSCs and BMSCs and examined their biological characteristics by comparative analyses. Although the iPSCs were more challenging to generate from the BMSCs than the AMSCs, both iPSC populations expressed pluripotent markers, such as stage-specific embryonic antigen (SSEA)-3, SSEA-4, tumour-related antigens (TRAs) TRA-1-60 and TRA-1-81, *OCT3/4* and *NANOG*. Furthermore, both cell populations differentiated well into three germ layer-derived cells, both *in vitro* and *in vivo*. These results indicate that iPSCs derived from frozen AMSCs/BMSCs exhibit equally acceptable iPSC characteristics and have potential in clinical applications as an alternative source of autogenous stem cells.**


**Received 2 July 2010; Accepted 13 March 2011**

**Keywords** **induced pluripotent stem cells; mesenchymal stem cells; somatic stem cells; embryonic stem cells; adipose tissue; bone marrow; regenerative medicine; tissue engineering**

## 1. Introduction

Mesenchymal stem cells (MSCs) are somatic stem cells found in various tissues, such as bone marrow, adipose tissue, tooth germ, synovial membranes and umbilical cord blood (Kern *et al.*, 2006), and are known to differentiate into hepatocytes, neurocytes, cardiomyocytes, osteocytes, chondrocytes and adipocytes (Salem *et al.*, 2009). Due to their wide differentiation potential, they are currently used in regenerative medicine (Salem *et al.*, 2009). Since 2001, we have utilized BMSCs for bone or cartilage regeneration in orthopaedic patients (Morishita *et al.*, 2006; Ohgushi *et al.*, 1999, 2005). MSCs are also found in adipose tissue, which is readily obtained by liposuction (Fraser *et al.*, 2006; Hayashi *et al.*, 2008), and the AMSCs have recently been used for various regenerative medical treatments (Garcia-Olmo *et al.*, 2003, 2005; Gimble *et al.*, 2003, 2007; Lendeckel *et al.*, 2004; Yoshimura *et al.*, 2008). It has been reported that both BMSCs and AMSCs show similar cell surface antigen patterns, although the cells have some characteristic differences. In particular, BMSCs exhibit a more extensive bone-forming

*Correspondence to: Shunsuke Yuba, Tissue Engineering Research Group, Health Research Institute, National Institute of Advanced Industrial Science and Technology (AIST), 3-11-46 Nakoji, Amagasaki, Hyogo 661-0974, Japan.
*E-mail: yuba-sns@aist.go.jp*

potential than AMSCs (Hayashi *et al.*, 2008). Therefore, BMSCs may be appropriate stem cells for bone tissue regeneration, whereas AMSCs may be used for treatments that do not require bone formation, such as heart repair. Concerning the clinical application of MSCs, their proliferation and differentiation potentials are limited and drastically decrease after several passages, resulting in a restriction of their application in regenerative medicine.

Alternatively, embryonic stem cells (ESCs) have unlimited proliferation and differentiation potential. However, disruption of an embryo is required to establish ESCs and thus their uses in medical applications elicit ethical concerns. Furthermore, because ESCs cannot be established from adult cells, it is impossible to make patient-derived ESCs to be used as autogenous grafts, which avoid transplantation rejection. In this regard, induced pluripotent stem cells (iPSCs) with unlimited proliferation and differentiation potential equivalent to ESCs have recently been established (Takahashi *et al.*, 2006, 2007; Yu *et al.*, 2007). Because iPSCs can be generated from somatic cells even after their terminal differentiation, iPSCs have been attracting attention as a new type of possible patient-derived autogenous stem cells for regenerative medicine. Many sources of adult cells in various tissues have been used for the generation of iPSCs, including skin fibroblasts, keratinocytes, blood cells (Patel *et al.*, 2010) and MSCs. Because harvesting, depository and transport methods of the MSCs have been established, usage of the cells is feasible for clinical applications. Notably, MSCs can be frozen/stocked for a long period with high viability (Kotobuki *et al.*, 2005). Due to the well-established characteristic features of MSCs, they are targeted as an ideal cell source for iPSC generation. In fact, we have previously reported the generation of iPSCs from frozen AMSCs (Aoki *et al.*, 2010). However, there are no comparative studies of the efficiency and biological activities of the iPSCs that are derived from BMSCs vs. from AMSCs. In this study, we established several lines of iPSCs from frozen stocks of BMSCs and AMSCs, and compared the efficiency of the iPSC generation, as well as differentiation potentials both *in vitro* and *in vivo*.

# 2. Materials and methods

## 2.1. FACs analysis

Cell surface antigens of BMSCs and AMSCs were analysed by flow cytometric analysis (FACS Calibur, BD Biosciences, Le Pont de Claix, France). Mouse anti-human monoclonal antibodies of FITC-conjugated CD13, CD14 CD44, CD45 (BioCarta, CA, USA), CD29, CD56, CD90, CD105 (AbD Serotec, NC, USA), CD31, CD34, HLA-I (Invitrogen), PE-conjugated CD73 (BD Bioscience) and CD133 (Miltenyi Biotec, Gladbach, Germany) were used. FITC- and PE-conjugated mouse IgG (Beckman Coulter, CA, USA) were used as negative controls.

## 2.2. *In vitro* osteogenic differentiation of BMSCs and AMSCs

MSCs were seeded at a density of $5 \times 10^3$ cells/cm$^2$ in a 12-well culture plate in minimum essential medium-$\alpha$ ($\alpha$-MEM; Invitrogen) containing 15% fetal bovine serum (FBS; JRH Biosciences, KS, USA) and cultured overnight. Next day, the medium was changed to osteogenic differentiation medium, which was supplemented with 10 mM $\beta$-glycerophosphate (Merck KGaA, Darmstadt, Germany), 0.07 mM L-ascorbic acid 2-phosphate magnesium salt *n*-hydrate (Wako) and 100 nM dexamethasone (Sigma). The medium was changed three times a week. As a control, the MSCs were also cultured in the medium without the ascorbic acid and dexamethasone.

After the osteogenic differentiation, the cells were used for assay for alkaline phosphatase (ALP) activity and ALP staining. For the ALP assay, the cells were washed with phosphate-buffered saline (PBS) and collected into a tube containing 500 µl TE buffer (pH 7.4, 1 mM EDTA and 100 mM NaCl). The cells in TE buffer were sonicated and 20 µl of the cell suspension was used to quantify DNA content, using Hoechst 33 258. Salmon sperm DNA (Life Technologies) was used as DNA standard. The sonicated cell suspension was centrifuged at 13 000 $\times$ *g* for 5 min at 4 °C, and 20 µl supernatant was used for ALP activity assay. *p*-Nitrophenylphosphate (pNPP; Zymed Laboratories, CA, USA) was used as the substrate, and the *p*-nitrophenol released during incubation for 30 min at 37 °C was measured. The ALP activity was normalized to DNA content (µmol/µg). ALP staining was done using an ALP Kit (Sigma) according to the manufacturer's instructions.

## 2.3. *In vitro* adipogenic differentiation of BMSCs and AMSCs

MSCs were seeded at a density of $2 \times 10^4$ cells/cm$^2$ in a 12-well culture plate in $\alpha$-MEM containing 15% FBS. The adipogenic differentiation was performed using the hMSC Differentiation Bullet Kit®, Adipogenid (PT-3004, Takara) according to the manufacturer's instructions. After adipogenic differentiation, the cells were fixed with 10% formaldehyde for 10 min at room temperature. The fixed cells were washed with 60% isopropanol and stained with oil red O solution for 15 min. The stained cells were washed with 60% isopropanol and PBS. As a control, the MSCs were also cultured in the medium without dexamethasone, indomethacin and 3-isobutyl-1-methylxanthine.

## 2.4. Plasmid construction

An open reading frame (ORF) cassette A (Invitrogen, Carlsbad, CA, USA) was introduced into the *Eco*RI site of the pMXs retroviral vector (Takahashi *et al.*, 2006). The ORFs of human *OCT3/4* (*POU5f1 isoform-1*), *SOX2*, *KLF4*

and *c-MYC* were amplified by RT–PCR and cloned into pENTR-D/TOPO (Invitrogen). All genes were transferred to the pMXs retroviral vector (kindly donated by Dr Kitamura), using Gateway Technology (Invitrogen) according to the manufacturer's instructions.

## 2.5. Cell culture

This study was approved by the ethics committee of the National Institute of Advanced Industrial Science and Technology. Culture expansion of BMSCs (0801TS33M A1/BMSC No. 1, P-2c AMS0422-PF57/BMSC No. 2 and 0702TS37M A2/BMSC No. 3) were carried out from frozen stocked BMSCs after informed consent of the donors had been obtained. Human AMSC lines (AMSC No. 1 and AMSC No. 3) were purchased from Invitrogen (lot numbers 1212 and 1199), and one line (AMSC No. 2) was from Lonza Biosciences (Gaithersburg, MD, USA; lot number 7F3890). The frozen BMSCs and AMSCs were thawed and used for the generation of iPSCs. Platinum-A (Plat-A) cells were purchased from Cell Biolabs (San Diego, CA, USA) (Takahashi *et al.*, 2007). SNL76/7 feeder cells were purchased from the European Collection of Cell Cultures (Salisbury, UK). BMSCs and AMSCs were maintained in $\alpha$-MEM containing 15% FBS, 100 U/ml penicillin and 100 μg/ml streptomycin (Invitrogen). Plat-A and SNL feeder cells were maintained in Dulbecco's modified Eagle's medium (DMEM; Invitrogen) containing 10% FBS, 100 U/ml penicillin and 100 μg/ml streptomycin. The iPSCs were generated and maintained in human ESC medium (D-MEM/F-12 with GlutaMAX-I; Invitrogen), supplemented with 20% knockout serum replacement (KSR; Invitrogen), 0.1 mM non-essential amino acids (Invitrogen), 0.1 mM 2-mercaptoethanol (Invitrogen), 100 U/ml penicillin, 100 μg/ml streptomycin and 5 ng/ml recombinant human basic fibroblast growth factor (bFGF; Wako, Osaka, Japan). MSCs, Plat-A and SNL76/7 feeder cells were passaged using 0.05% trypsin/0.53 mM EDTA (Invitrogen). The iPSCs were passaged using dissociation solution [0.25% trypsin (Invitrogen), 0.1 mg/ml collagenase type IV (Invitrogen), 10 mM $CaCl_2$ (Wako) and 20% KSR in distilled water]. The parental cells of these MSCs were free from bacterial, fungal and mycoplasma contamination because primary cultures of BMSCs were done in the clean room at our cell-processing centre and AMSC lines were obtained from the companies with certification. We also performed microbiological tests several times during the culture; furthermore, we have a system to avoid cross-contamination during iPSCs generation, evidenced by short tandem repeat (STR) profile analysis of genomic DNA (Aoki *et al.*, 2010).

## 2.6. Retroviral production

Plat-A packaging cells were seeded at $8 \times 10^6$ cells/100 mm dish and cultured overnight. The next day, pMXs retroviral vectors containing the ORFs of human *OCT3/4, SOX2, KLF4* and *c-MYC* were transfected into Plat-A cells using the FuGENE HD Transfection Reagent (Roche Diagnostics, Basel, Switzerland). Viral supernatants were collected 48 and 72 h post-transfection, then filtered through a 0.45 μm pore-size filter and supplemented with 4 mg/ml Polybrene (Sigma, St. Louis, MO, USA). The MSCs were transduced with a *OCT3/4:SOX2:KLF4:c-MYC* = 1:1:1:1 mixture of viral supernatant.

## 2.7. Generation of iPSCs

BMSCs and AMSCs were seeded at $5 \times 10^4$ cells/100 mm dish and cultured overnight. At this time, the passage numbers of BMSC nos 1, 2 and 3 and AMSC nos 1, 2 and 3 were P5, P7, P7, P6, P8 and P7, respectively. After the overnight culture, the culture medium was changed to viral supernatant and cultured for 24 h, then the viral supernatant was changed to fresh viral supernatant and cultured for an additional 24 h. The viral supernatant was changed to $\alpha$-MEM containing 15% FBS with a daily medium change. After 3 days, the viral infected cells were seeded on SNL feeder cells at $5 \times 10^3$–$5 \times 10^5$ cells/100 mm dish. The next day, the medium was changed to human ESC medium containing valproic acid (VPA; Wako). The medium was changed every other day for 2 weeks, then cultured without VPA. From 7 to 24 days post-infection, colonies were selected based on human ESC-like colony morphology. The selected colonies were subsequently expanded and maintained on SNL feeder cells in human ESC medium. Cells were always cultured in a humidified atmosphere of 95% air with 5% $CO_2$ at 37 °C. Reprogramming efficiency was determined as the number of total human ESC-like colonies per total number of infected cells.

## 2.8. RNA isolation and reverse transcription

Total RNA was isolated using an RNeasy Mini Kit (Qiagen, Hilden, Germany) and treated with a TURBO DNA-free™ kit (Applied Biosystems, Foster City, CA, USA), according to the manufacturer's instructions. Total RNA (1 μg) was used for cDNA synthesis, using a ReverTra Ace-$\alpha$™ kit (Toyobo, Osaka, Japan) and oligo(dT) 20 primers. PCR was performed using an ExTaq HS™ kit (Takara Bio, Shiga, Japan). Primer sequences are shown in Table 3.

## 2.9. Alkaline phosphatase (ALP) staining and immunofluorescence microscopy

ALP staining was performed using a Leukocyte ALP Kit (Sigma) according to the manufacturer's instructions. For immunofluorescent microscopy, cells were fixed with PBS containing 4% paraformaldehyde for 10 min at room temperature. After washing with PBS, the cells were treated with PBS containing 0.1% Triton X-100 for 10 min and then 1% bovine serum albumin (BSA, A2153, Sigma) for 10 min at room temperature. The cells were incubated

Table 1. Analyses of cell surface antigens on BMSCs and AMSCs

| | Cell surface antigen (%) | | | | | | | | | | | | | |
|---|---|---|---|---|---|---|---|---|---|---|---|---|---|---|
| MSC line | CD13 | CD14 | CD29 | CD31 | CD34 | CD44 | CD45 | CD56 | CD73 | CD90 | CD105 | CD133 | HLA-DR | HLA-I |
| BMSC No.1 | 97.30 | 2.88 | 99.92 | 2.12 | 1.73 | 98.89 | 1.86 | 4.09 | 99.9 | 99.85 | 99.57 | 0.65 | 0.25 | 99.75 |
| BMSC No.2 | 99.26 | 2.15 | 99.98 | 2.16 | 1.41 | 99.74 | 1.67 | 5.10 | 99.27 | 99.94 | 99.67 | 0.52 | 0.52 | 99.79 |
| BMSC No.3 | 99.52 | 3.25 | 99.98 | 2.52 | 1.01 | 99.75 | 2.44 | 6.96 | 99.87 | 100.0 | 99.95 | 5.76 | 0.61 | 99.82 |
| AMSC No.1 | 99.67 | 1.53 | 99.71 | 1.36 | 1.11 | 98.59 | 1.09 | 1.26 | 99.93 | 99.96 | 98.01 | 0.57 | 0.57 | 86.35 |
| AMSC No.2 | 99.97 | 1.18 | 99.98 | 1.66 | 0.71 | 99.93 | 0.99 | 2.38 | 99.71 | 99.98 | 99.93 | 0.48 | 0.46 | 99.28 |
| AMSC No.3 | 99.99 | 3.61 | 99.97 | 2.91 | 2.03 | 99.95 | 2.79 | 2.89 | 99.89 | 99.99 | 99.96 | 0.51 | 0.70 | 96.98 |

Table 2. Efficiency of iPSC generation from BMSCs and AMSCs

| Parental cells | Passage No. | Number of colony | Reprogramming efficiency |
|---|---|---|---|
| BMSC No.1 (0801TS33MA1) | P5 | 8 | 0.0008 |
| BMSC No.2 (P-2cAMS0422-PF57) | P7 | 1 | 0.0002 |
| BMSC No.3 (0702TS37MA2) | P7 | 0 | 0 |
| AMSC No.1 (Invitrogen #1212) | P6 | 88 | 0.0293 |
| AMSC No.2 (Lonza #7F3890) | P8 | 31 | 0.0022 |
| AMSC No.3 (Invitrogen #1199) | P7 | 5 | 0.0005 |

No statistically significant differences between BMSCs and AMSCs by Mann–Whitney U-test and $\chi^2$ test, probably due to small sample size.

with a primary antibody overnight at 4 °C, washed and incubated with a secondary antibody for 30 min. The primary antibodies used were SSEA-3 (1:200, MAB4303; Millipore, Billerica, MA, USA), SSEA-4 (1:200, MAB4304; Millipore), TRA-1-60 (1:200, ab16288-200; Abcam, Cambridge, UK), TRA-1-81 (1:200, ab16289-200; Abcam), OCT4 (1:200, ab19857-100; Abcam), NANOG (1:50, ab21624; Abcam), SOX17 (1:200, AF1924; R&D Systems, Minneapolis, MN, USA), α-smooth muscle actin (pre-diluted, N1584; Dako, Glostrup, Denmark) and βIII-tubulin (1:200, CBL412; Millipore). Secondary antibodies used were from the Invitrogen AlexaFluor series (1:300). Nuclei were detected with 0.2 μg/ml Hoechst 33 342 (Molecular Probes, Eugene, OR, USA).

### 2.10. *In vitro* differentiation

For embryoid body (EB) formation, human ESC-like colonies were harvested by treatment with dissociation solution and transferred to a low attachment culture dish (Prime Surface; Sumitomo Bakelite, Tokyo, Japan) in human ESC medium without recombinant bFGF. The medium was changed every other day. After 9–12 days of floating culture, EBs were found and transferred onto gelatin-coated plates for an additional 10 days of culture in the same medium.

### 2.11. Teratoma formation

Clumps of ESC-like colonies from one 100 mm dish were suspended in 60 μl human ESC medium without human recombinant bFGF. The cell clump suspension (25 μl) was injected into each testis of a severe combined immunodeficient (SCID) mouse. Tumours were collected 8–12 weeks after injection and fixed with 10% paraformaldehyde. The paraffin-embedded tumours were sectioned and stained with haematoxylin and eosin (H&E).

### 2.12. Karyotype analysis

Chromosomal G-band analyses and multicolour Fluorescence in situ hybridization (FISH) were performed at the Nihon Gene Research Laboratories (Sendai, Japan). At this time, the passage numbers of BMSC nos 1 and 2 and AMSC nos1, 2 and 3 were P7, P12, P11, P9 and P9, respectively.

## 3. Results

### 3.1. FACs analysis of MSCs

Three lines of BMSCs and AMSC no. 2 were analysed by flow cytometry (Table 1). These numbers in Table 2 represent the percentages of marker-positive cells. All cell lines were positive for well-known mesencymal markers, such as CD13, CD29, CD44, CD73, CD90, CD105 and HLA-I. Meanwhile, they were negative for CD14, CD31, CD34, CD45, CD56 and CD133. These data indicate that these MSC lines were mesenchymal-type cells.

### 3.2. Differentiation analysis of MSCs

We examined the differentiation potentials of these MSCs from BMSCs and AMSCs. When three lines of BMSCs and

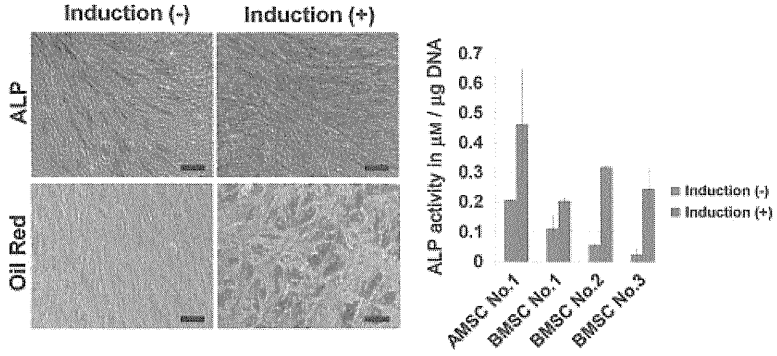


Figure 1. Osteogenic and adipogenic differentiation potential of BMSCs and AMSCs. MSCs were cultured with (induction$^{+}$) or without (induction$^{-}$) differentiation medium. ALP as a marker of osteogenic differentiation and oil red stain as a maker of adipogenic differentiation are seen in figures at left. Scale bars = 200 μm. ALP activity measurements are seen in figure at right

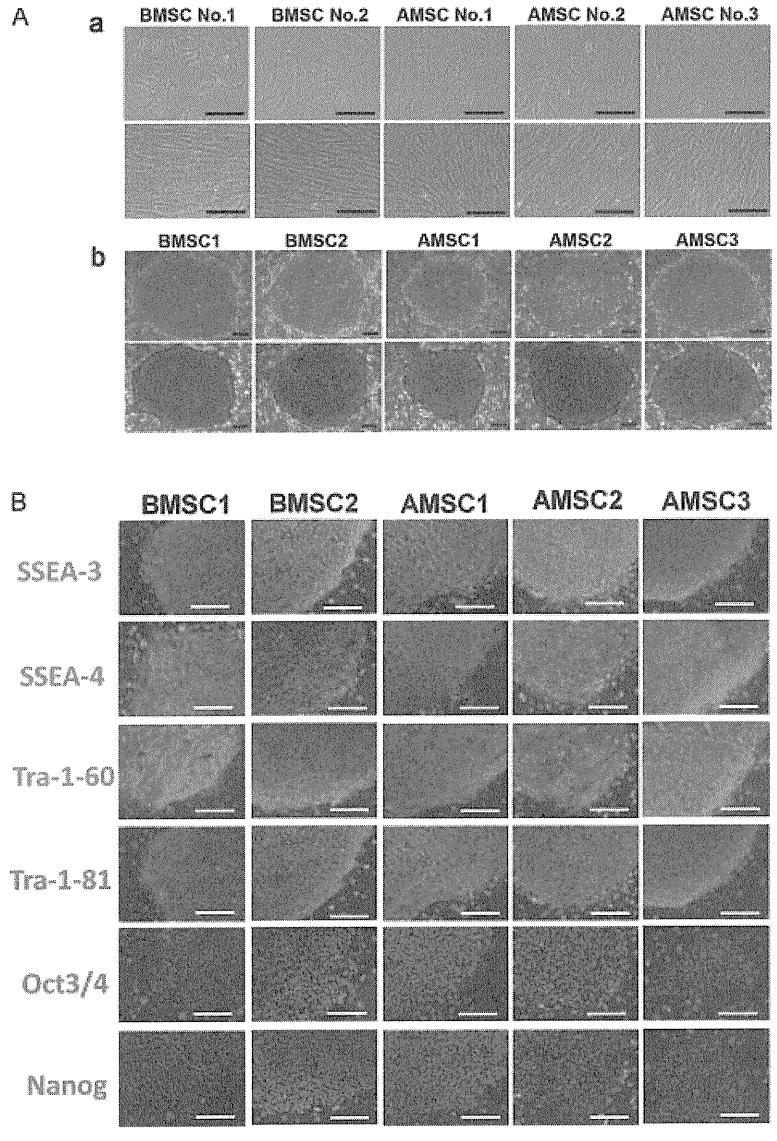


Figure 2. Morphology of the parental cells of BMSCs (BMSC nos 1 and 2) and AMSCs (AMSC nos 1–3) and ESC-like colonies (BMSC nos 1 and 2 and AMSC nos 1–3) from the corresponding parental cells. (A) (a) Typical microscopic view of parental cells at low density (upper) and high density (lower); (b) ESC-like colonies before (upper) and after (lower) ALP staining. Scale bar = 200 μm. (B) Immunofluorescent microscopy of ESC-like colonies for SSEA-3, SSEA-4, TRA-1-60, TRA-1-81, OCT3/4 and NANOG. Nuclei were stained with Hoechst 33342. Scale bar = 200 μm


*J Tissue Eng Regen Med* 2012;6: 261–271.
DOI: 10.1002/term

AMSC no. 1 were cultured with osteogenic differentiation medium, all MSCs showed strong ALP staining and high ALP activity (upper left and right panels in Figure 1). Likewise, when cultured with adipogenic differentiation medium, these MSCs showed positive staining for oil red O (lower left panels in Figure 1). These data showed that all MSCs used for iPSCs generation had at least osteogenic and adipogenic differentiation potentials.

## 3.3. Generation of iPSCs from BMSCs and AMSCs

After approximately 22 days from the viral infection, we found several colonies displaying human ESC-like morphologies. The ratio of the number of colony formations (i.e. the reprogramming efficiency) in the BMSCs (nos 1, 2 and 3) and AMSCs (nos 1, 2 and 3) were 0.0008%, 0.0002%, 0%, 0.0293%, 0.0022% and 0.0005%, respectively (Table 2). Some of the human ESC-like colonies were selected, expanded for several passages (Figure 2Ab) and then stained for ALP activity. Almost all the colonies showed high ALP activity (Figure 2Ab). The data in the following sections were obtained from the putative ESC-like colonies derived from the corresponding culture-expanded MSCs. For example, the colonies named BMSC1 and AMSC3 were derived from BMSC no. 1 and AMSC no. 3, respectively.

## 3.4. Characterization of iPSCs from BMSCs and AMSCs

To confirm that the colonies derived from the BMSCs and AMSCs contained authentic iPSCs, we evaluated human ESC marker expressions, using immunofluorescent microscopy and RT–PCR. Immunofluorescent microscopy showed that the colonies expressed the following human ESC-specific surface antigens: stage-specific embryonic antigen (SSEA)-3; SSEA-4; tumour-related antigen (TRA)-1-60; and TRA-1-81. The cells also showed the ESC-specific transcription factors, *OCT3/4* and *NANOG* (Figure 2B).

RT–PCR analysis showed that the colonies expressed human ESC marker genes *OCT3/4, SOX2, NANOG*, reduced expression 1 (*REX1*), undifferentiated embryonic cell transcription factor 1 (*UTF1*), growth and differentiation factor 3 (*GDF3*), developmental pluripotency associated 2 (*DPPA2*), *DPPA4, DPPA5* and telomerase reverse transcriptase (*TERT*). The retroviral transgenes (Tg) of *Tg-OCT3/4, Tg-SOX2* and *Tg-MYC* were not expressed, and a trace of Tg-KLF4 was detected in the colonies (Figure 3).

## 3.5. EB formation and *in vitro* differentiation

To examine differentiation potential, we induced EB formation. After 9–12 days of floating culture of the dissociated cells from ESC-like colonies, the cells formed

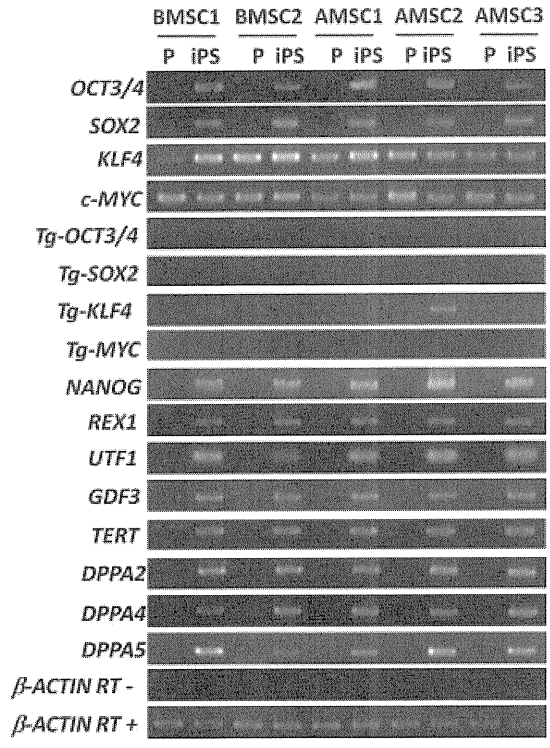


**Figure 3. RT–PCR analysis of expressions of ESC marker genes, endogenous *KLF4* and *c-MYC*, and retroviral transgenes (Tg). P, parental cells**

spherical structures (EBs; Figure 4A). The EBs were transferred onto gelatin-coated plates and cultured for an additional 9–12 days. Immunofluorescence microscopy showed that the cells were *β*III-*tubulin*- (a marker of ectoderm), *α-smooth muscle actin*- (*α-SMA*, mesoderm), *Vimentin*- (mesoderm and parietal endoderm) and *SOX17* (endoderm)-positive (Figure 4A). RT–PCR analysis confirmed that the cells expressed *MAP2, PAX6* (endoderm), *TNTC, BRACHURY, FOXA2* (mesoderm), *SOX17* and *AFP* (endoderm) (Figure 4B). These data imply that the ESC-like colonies had the potential to differentiate into various cells of the three germ layers *in vitro*.

## 3.6. Teratoma formation

To identify *in vivo* pluripotency, we injected the colonies from the AMSCs and BMSCs into the testes of SCID mice. We used three or four mice for each MSC cell line. More than half of the testes showed tumour formations 8–12 weeks after injection. Histological examination of the tumours revealed tissues representative of the three germ layers: gut-like epithelium (endoderm), cartilage (mesoderm) and neuroepithelial rosettes (ectoderm) (Figure 5). These findings indicate that the tumours were teratoma formations. Thus, the colonies from the BMSCs and AMSCs had the potential to differentiate into the three germ layers *in vivo*.

Collectively, the *in vitro* and *in vivo* data confirmed that the ESC-like colonies obtained after retroviral transduction of *OCT3/4, SOX2, KLF4* and *c-MYC* into either AMSCs or BMSCs were indeed authentic iPSCs.

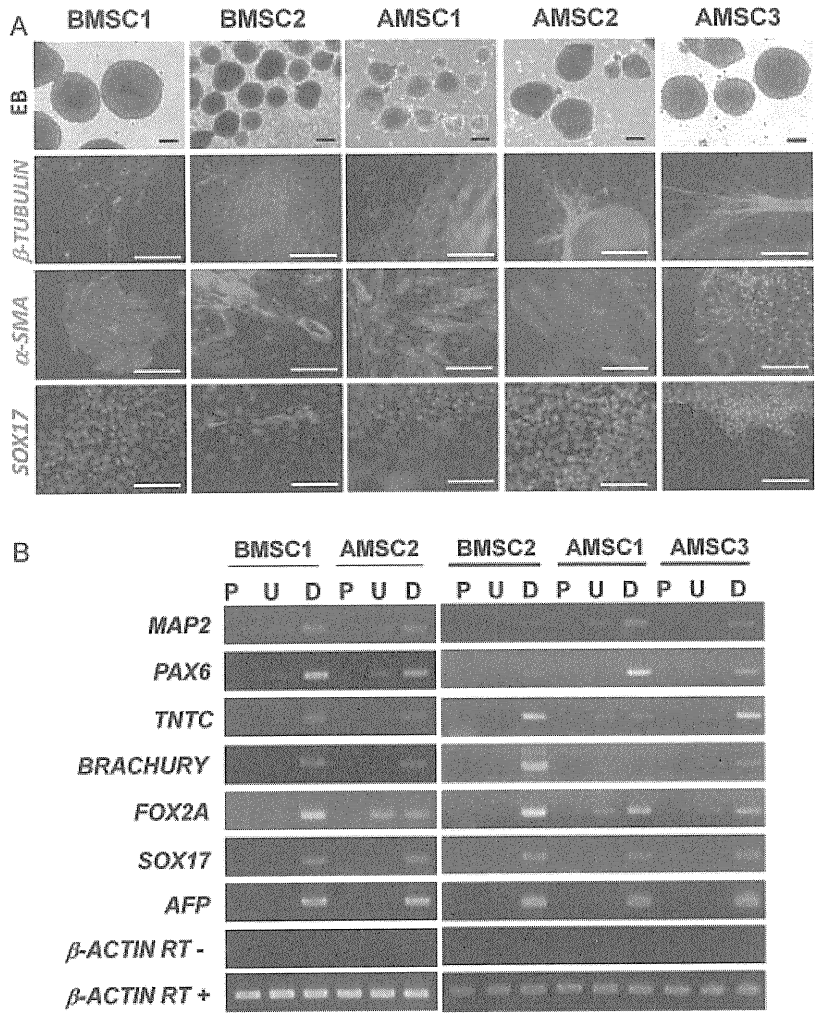


Figure 4. *In vitro* differentiation of ESC-like colonies from BMSCs and AMSCs. (A) EB formation. Immunofluorescent microscopy showing βIII-tubulin (green), α-SMA (green) and SOX17 (red). Nuclei were stained with Hoechst 33342. Scale bars = 200 μm. (B) RT–PCR analysis of expressions of differentiation marker genes: *MAP2, PAX6* (ectoderm), *TNTC, BRACHURY, FOXA2* (mesoderm), *SOX17* and *AFP* (endoderm). P, parental cells; U, undifferentiated cells; and D, differentiated cells via EB

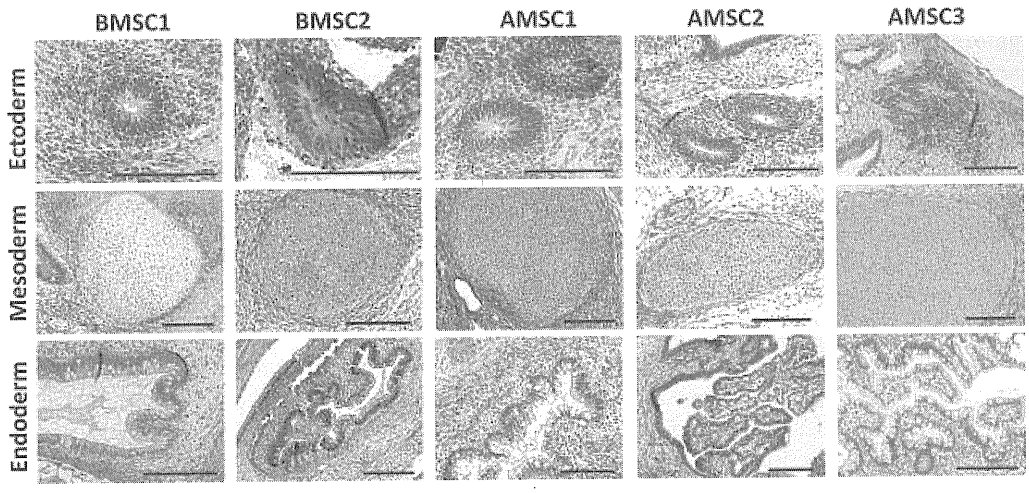


Figure 5. Teratoma formations of ESC-like colonies from BMSCs and AMSCs after their injection into mice testes. H&E staining showed neuroepithelial rosettes (ectoderm), cartilage (mesoderm) and gut-like epithelium (endoderm)

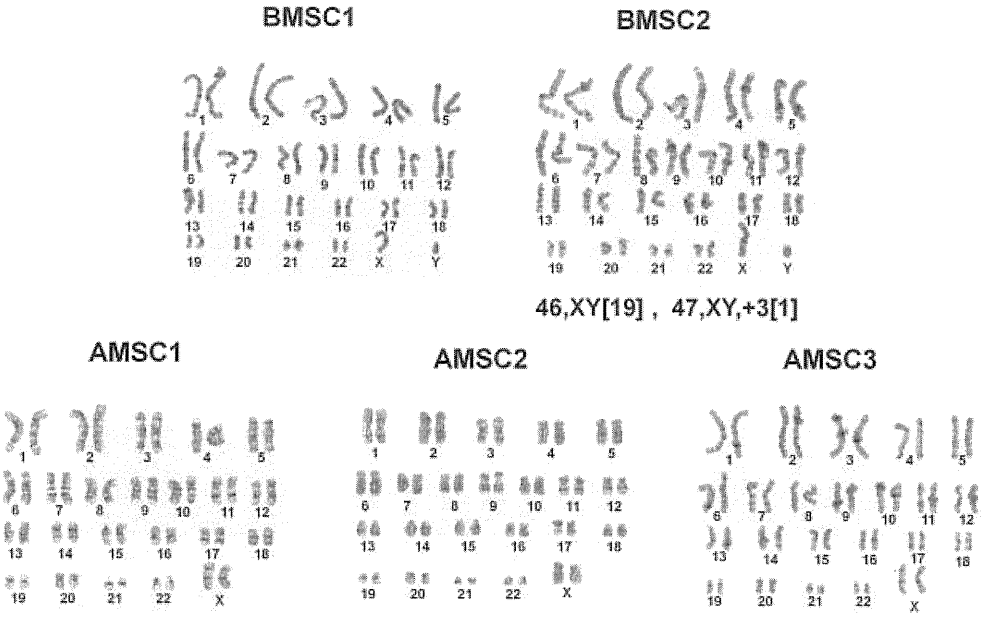


**Figure 6.** Karyotype (G-band) analyses of ESC-like colonies from BMSCs and AMSCs. BMSC1, AMSC1, AMSC2 and AMSC3 showed normal karyotypes. BMSC2 showed a partially abnormal karyotype

### 3.7. Karyotype analysis

We performed karyotype investigations by chromosomal G-band analysis (Figure 6) and multicolour FISH analysis (data not shown). Four lines of iPSCs of BMSC1, AMSC1, AMSC2 and AMSC3 showed normal karyotypes. BMSC2 showed chromosome 3 trisomy in only one cell out of 20 cells investigated.

## 4. Discussion

In the first report of mouse iPSC generation, the authors generated iPSCs using four transcription factors (*OCT3/4, SOX2, KLF4* and *c-MYC*) (Takahashi *et al.*, 2006). In 2007, they also generated human iPSCs using the same set of four factors (Takahashi *et al.*, 2007). Simultaneously, other investigators generated human iPSCs using another set of four factors (*OCT3/4, SOX2, NANOG* and *LIN28*) (Yu *et al.*, 2007). Since then, iPSC generation using three transcription factors (*OCT3/4, SOX2* and *KLF4*) without *c-MYC* (an oncogene) has been reported (Nakagawa *et al.*, 2008; Wernig *et al.*, 2008). Utilization of neural stem cells (NSCs) as a cell source resulted in successful iPSC generation using two transcription factors (*OCT3/4* and *KLF4* or *OCT3/4* and *c-MYC*) (Kim *et al.*, 2008). Furthermore, the same group also reported the generation of mouse, as well as human, iPSCs from MSCs using only one factor, *OCT3/4* (Kim *et al.*, 2009b, 2009c). Based on these reports, it is possible to decrease the number of transcription factors for iPSC generation by the selection of the parental cell source. In particular, cells having characteristic features of 'stemness' might be valuable for iPSC generation.

Various tissues in the human body contain MSCs. Although their proliferation/differentiation potentials are much less than those of ESCs and iPSCs, MSCs are adult cells and thus useful for clinical applications in regenerative medicine. As such, we have used BMSCs for bone/cartilage regeneration. We speculate that the proliferation/differentiation limitations of MSCs may be overcome by generation of iPSCs from MSCs. In our preliminary experiments, we transduced three transcription factors (*OCT3/4, SOX2* and *KLF4*) without *c-MYC* into human BMSCs; however it was extremely difficult to detect the iPSC-like colonies. Because MSCs also reside in adipose tissue, we then successfully generated iPSCs from AMSCs, using the same three factors (Aoki *et al.*, 2010). If BMSC-derived iPSCs have genuine iPSC properties, they could be useful for clinical applications despite their low efficiency of iPSC generation, because the iPSCs will have an infinite proliferative potential. In this study, we tried to generate iPSCs from both AMSCs and BMSCs using four transcription factors (*OCT3/4, SOX2, KLF4* and *c-MYC*), and we examined cellular biological characteristics by comparative analyses.

We determined the efficiency of iPSC generation from AMSCs and BMSCs using four factors. We found that the total number of ESC-like colonies in the AMSCs was more than that in the BMSCs, indicating a higher tendency of iPSC generation potential in AMSCs than in BMSCs (Table 2). We recently reported upregulation of some genes regarding DNA repair/histone conformational change in the high iPSC generation cells of mesenchymal types (Oda *et al.*, 2010). Difference of the gene expression profiles between AMSCS and BMSCs might be seen, although further extensive studies are needed to confirm this assumption. We also examined whether the obtained ESC-like colonies had sufficient pluripotent properties. Cells in the colonies from both BMSCs and AMSCs exhibited a human ESC-like morphology

Table 3. PCR primers

| Primer | Sequence (5′ to 3′) | Applications | Tm |
|---|---|---|---|
| hOCT4–S842 | CTGCAGCAGATCAGCCACATCGCCCAGCAG | OCT3/4 endo and transgene RT–PCR | 73 |
| hOCT4–AS1283 | CTTCCCTCCAACCAGTTGCCCCAAAC | Endo OCT3/4 RT–PCR | 65 |
| hSOX2–S1430 | GGGAAATGGGAGGGGTGCAAAAGAGG | | 65 |
| | | Endo SOX2 RT–PCR | |
| hSOX2–AS1555 | TTGCGTGAGTGTGGATGGGATTGGTG | | 63 |
| hSOX2–S1004 | CAGATGCAGCCCATGCACCGCTACGACGTG | SOX2 transgene RT–PCR | 73 |
| hKLF4–S1457 | ACGATCGTGGCCCCGGAAAAGGACC | KLF4 endo and transgene RT–PCR | 67 |
| hKLF4–AS1826 | TGATTGTAGTGCTTTCTGGCTGGGCTCC | Endo KLF4 RT–PCR | 65 |
| pMXs–AS3201 | TAAAATCTTTTATTTTATCGTCGACCACTG | Transgene RT–PCR | 53 |
| hMYC–S253 | GCGTCCTGGGAAGGGAGATCCGGAGC | | 71 |
| | | c–MYC transgene RT–PCR | |
| hMYC–AS555 | TTGAGGGGCATCGTCGCGGGAGGCTG | | 71 |
| hMYC–S1580 | CAACAACCGAAAATGCACCAGCCCCAG | c–MYC transgene RT–PCR | 65 |
| hNANOG–S968 | CAGCCCCGATTCTTCCACCAGTCCC | | 67 |
| | | NANOG RT–PCR | |
| hNANOG–AS1334 | CGGAAGATTCCCAGTCGGGTTCACC | | 65 |
| hREX1–S | CAGATCCTAAACAGCTCGCAGAAT | | 57 |
| | | RET1 RT–PCR | |
| hREX1–AS | GCGTACGCAAATTAAAGTCCAGA | | 55 |
| hUTF1–S832 | CCGTCGCTGAACACCGCCCTGCTG | | 69 |
| | | UTF1 RT–PCR | |
| hUTF1–AS979 | CGCGCTGCCCAGAATGAAGCCCAC | | 67 |
| hGDF3–S243 | CTTATGCTACGTAAAGGAGCTGGG | | 59 |
| | | GDF3 RT–PCR | |
| hGDF3–AS850 | GTGCCAACCCAGGTCCCGGAAGTT | | 65 |
| hDPPA2–S85 | CCGTCCCCGCAATCTCCTTCCATC | | 65 |
| | | DPPA2 RT–PCR | |
| hDPPA2–AS667 | ATGATGCCAACATGGCTCCCGGTG | | 63 |
| hDPPA4–S532 | GGAGCCGCCTGCCCTGGAAAATTC | | 65 |
| | | DPPA4 RT–PCR | |
| hDPPA4–AS916 | TTTTTCCTGATATTCTATTCCCAT | | 49 |
| hDPPA5–S40 | ATATCCCGCCGTGGGTGAAAGTTC | | 61 |
| | | DPPA5 RT–PCR | |
| hDPPA5–AS259 | ACTCAGCCATGGACTGGAGCATCC | | 63 |
| hAFP–S948 | GAATGCTGCAAACTGACCACGCTGGAAC | | 65 |
| | | AFP RT–PCR | |
| hAFP–AS1201 | TGGCATTCAAGAGGGTTTTCAGTCTGGA | | 61 |
| hSOX17–S423 | CGCTTTCATGGTGTGGGCTAAGGACG | | 65 |
| | | SOX17 RT–PCR | |
| hSOX17–AS583 | TAGTTGGGGTGGTCCTGCATGTGCTG | | 65 |
| hFOXA2–S208 | TGGGAGCGGTGAAGATGGAAGGGCAC | | 67 |
| | | FOXA2 RT–PCR | |
| hFOXA2–AS398 | TCATGCCAGCGCCCACGTACGACGAC | | 69 |
| hBRACHYURY–S1292 | GCCCTCTCCCTCCCCTCCACGCACAG | | 73 |
| | | BRACHYURY RT–PCR | |
| hBRACHYURY–AS1540 | CGGCGCCGTTGCTCACAGACCACAGG | | 71 |
| hTNTC–S524 | ATGAGCGGGAGAAGGAGCGGCAGAAC | | 67 |
| | | TNTC RT–PCR | |
| hTNTC–AS730 | TCAATGGCCAGCACCTTCCTCCTCTC | | 65 |
| hMAP2–S5401 | CAGGTGGCGGACGTGTGAAAATTGAGAGTG | | 67 |
| | | MAP2 RT–PCR | |
| hMAP2–AS5587 | CACGCTGGATCTGCCTGGGGACTGTG | | 69 |
| hPAX6–S1206 | ACCCATTATCCAGATGTGTTTGCCCGAG | | 63 |
| | | PAX6 RT–PCR | |
| hPAX6–AS1497 | ATGGTGAAGCTGGGCATAGGCGGCAG | | 67 |
| human beta–actin F | AGAAAATCTGGCACCACAC | | 53 |
| | | $\beta$–ACTIN RT–PCR | |
| human beta–actin R | CTCCTTAATGTCACGCACG | | 55 |

(Figure 2Ab), and the colonies exhibited high ALP activity (Figure 2Ab) as well as expressions of undifferentiated markers (Figures 2B, 3). Concerning the differentiation potentials of the ESC-like colonies, we made EBs from the colonies and demonstrated that the cells in the EBs differentiated well into three germ layer-derived cells. The *in vitro* differentiation potentials were also confirmed by *in vivo* transplantation of the ESC-like colonies into mouse testes. Histological findings of the transplants showed gut-like epithelium (endoderm), cartilage (mesoderm) and neuroepithelial rosettes (ectoderm) (Figure 5). The *in vitro*, as well as *in vivo*, differentiation potentials were well demonstrated using parental cells of both BMSCs and AMSCs. Collectively, these results indicate that the ESC-like colonies derived from both BMSCs and AMSCs were iPSCs, although there was a difference in the efficiency of iPSC generation.

The low generation efficiency of BMSCs may be improved by using other factors in the process of iPSC generation. It has been reported that small molecule compounds, such as histone deacetylase inhibitor (Huangfu *et al.*, 2008), GSK3 inhibitor (Li *et al.*, 2009), TGF$\beta$ signalling inhibitor (Lin *et al.*, 2009) and butyric acid (Mali *et al.*, 2010) enhance iPSC generation. We used *c-MYC* for iPSC generation, particularly for iPSC generation from BMSCs. *c-MYC* is a known oncogene, and Okita *et al.* (2007) reported that iPSCs can give rise to cancer by re-expression of the *c-MYC* transgene. This problem, which is crucial for clinical application, might be solved by using the Sendai virus method without insertion of transgenes into the genome (Fusaki *et al.*, 2009) or a protein transduction method without gene transfection (Kim *et al.*, 2009a; Zhou *et al.*, 2009).

One of the significant findings of this study was that we could generate iPSCs from frozen/stocked MSCs. According to our experience, MSCs can be stocked for several years, even at $-80\,^{\circ}C$, with high cell viability (Kotobuki *et al.*, 2005). In the future, we will provide regenerative medicine using patients' MSCs and at the same time we will stock some of the MSCs. If the MSC therapy is not effective by their proliferation/differentiation limitations, it will be possible to use iPSCs generated from the stocked MSCs. For clinical applications of iPSCs, we should consider possible complications, such as tumourigenicity of iPSCs, because iPSC transplantation can cause teratoma formation. Miura *et al.* (2009) reported that iPSC-derived secondary neurosphere transplantation to the striatum of a NOD/SCID mouse caused tumour formations. Interestingly, the frequency of the teratoma formation was related to the number of undifferentiated cells that resided in their preparation. Consequently, if undifferentiated cells can be removed, the tumourigenicity might be prevented. Indeed, there are methods to remove undifferentiated cells, and therefore clinical application of human iPSCs derived from MSCs might be possible in the future. The application could be done using differentiated cells of interest derived from the iPSCs and some have already reported differentiation methods towards neural cells (Vierbuchen *et al.*, 2010) and beating cardiomyocites (Ieda *et al.*, 2010). Interestingly, these differentiations from adult cells without iPS generation can be done. Vierbuchen *et al.* (2010) converted dermal fibroblasts to functional neurons using three factors (Ascl1, Brn2 and Myt1l) and Ieda *et al.* (2010) generated beating cardiomyocytes using three factors (Gata4, Mef2c and Tbx5). These direct reprogramming methods might be alternative methods to show functional differentiation from adult cells and circumvent the tumourigeneicity.

In conclusion, BMSCs tended to show a lower efficiency in the generation of iPSCs than AMSCs; however, iPSCs derived from both AMSCs and BMSCs exhibited equal differentiation potentials into cells of three germ layers. Therefore, we believe iPSCs generated from BMSCs or AMSCs can be used as patient-derived autogenous stem cells, although further studies are needed for consideration of clinical applications.

## Acknowledgements

We warmly thank Dr Toshio Kitamura for providing the retroviral system. We also thank our colleagues in the Tissue Engineering Group, Health Research Institute, National Institute of Advanced Industrial Science and Technology (AIST). This work was partly supported by the Project for Realization of Regenerative Medicine from the Ministry of Education, Culture, Sports, Science and Technology of Japan. The study sponsors had no role in the study design, data analysis or data interpretation, or in the writing of the report.

# References

Aoki T, Ohnishi H, Oda Y, *et al.* 2010; Generation of induced pluripotent stem cells from human adipose-derived stem cells without c-MYC. *Tissue Eng A* **16:** 2197–2206.

Ieda M, Fu JD, Delgado-Olguin P, *et al.* 2010; Direct reprogramming of fibroblasts into functional cardiomyocytes by defined factors. *Cell* **142:** 375–386.

Fraser JK, Wulur I, Alfonso Z, *et al.* 2006; Fat tissue: an underappreciated source of stem cells for biotechnology. *Trends Biotechnol* **24:** 150–154.

Fusaki N, Ban H, Nishiyama A, *et al.* 2009; Efficient induction of transgene-free human pluripotent stem cells using a vector based on Sendai virus, an RNA virus that does not integrate into the host genome. *Proc Jpn Acad Ser B Phys Biol Sci* **85:** 348–362.

Garcia-Olmo D, Garcia-Arranz M, Garcia LG, *et al.* 2003; Autologous stem cell transplantation for treatment of rectovaginal fistula in perianal Crohn's disease: a new cell-based therapy. *Int J Colorectal Dis* **18:** 451–454.

Garcia-Olmo D, Garcia-Arranz M, Herreros D, *et al.* 2005; A phase I clinical trial of the treatment of Crohn's fistula by adipose mesenchymal stem cell transplantation. *Dis Colon Rectum* **48:** 1416–1423.

Gimble JM, 2003; Adipose tissue-derived therapeutics. *Expert Opin Biol Ther* **3:** 705–713.

Gimble JM, Katz AJ, Bunnell BA, *et al.* 2007; Adipose-derived stem cells for regenerative medicine. *Circ Res* **100:** 1249–1260.

Hayashi O, Katsube Y, Hirose M, *et al.* 2008; Comparison of osteogenic ability of rat

mesenchymal stem cells from bone marrow, periosteum, and adipose tissue. *Calcif Tissue Int* **82:** 238–247.

Huangfu D, Osafune K, Maehr R, *et al.* 2008; Induction of pluripotent stem cells from primary human fibroblasts with only Oct4 and Sox2. *Nat Biotechnol* **26:** 1269–1275.

Kim D, Kim CH, Moon JI, *et al.* 2009a; Generation of human induced pluripotent stem cells by direct delivery of reprogramming proteins. *Cell Stem Cell* **4:** 472–476.

Kim JB, Greber B, Arauzo-Bravo MJ, *et al.* 2009b; Direct reprogramming of human neural stem cells by OCT4. *Nature* **461:** 649–653.

Kim JB, Sebastiano V, Wu G, *et al.* 2009c; Oct4-induced pluripotency in adult neural stem cells. *Cell* **136:** 411–419.

Kim JB, Zaehres H, Wu G, *et al.* 2008; Pluripotent stem cells induced from adult neural stem cells by reprogramming with two factors. *Nature* **454:** 646–650.

Kern S, Eichler H, Stoeve J, *et al.* 2006; Comparative analysis of mesenchymal stem cells from bone marrow, umbilical cord blood, or adipose tissue. *Stem Cells* **24:** 1294–1301.

Kotobuki N, Hirose M, Machida H, *et al.* 2005; Viability and osteogenic potential of cryopreserved human bone marrow-derived mesenchymal cells. *Tissue Eng* **11:** 663–673.

Lendeckel S, Jodicke A, Christophis P, *et al.* 2004; Autologous stem cells (adipose) and fibrin glue used to treat widespread traumatic calvarial defects: case report. *J Craniomaxillofac Surg* **32:** 370–373.

Li W, Zhou H, Abujarour R, *et al.* 2009; Generation of human-induced pluripotent stem cells in the absence of exogenous Sox2. *Stem Cells* **27:** 2992–3000.

Lin T, Ambasudhan R, Yuan X, 2009; A chemical platform for improved induction of human iPSCs. *Nat Methods* **6:** 805–808.

Mali P, Chou BK, Yen J, *et al.* 2010; Butyrate greatly enhances derivation of human induced pluripotent stem cells by promoting epigenetic remodeling and the expression of pluripotency-associated genes. *Stem Cells* **28:** 713–720.

Miura K, Okada Y, Aoi T, *et al.* 2009; Variation in the safety of induced pluripotent stem cell lines. *Nat Biotechnol* **27:** 743–745.

Morishita T, Honoki K, Ohgushi H, *et al.* 2006; Tissue engineering approach to the treatment of bone tumors: three cases of cultured bone grafts derived from patients' mesenchymal stem cells. *Artif Organs* **30:** 115–118.

Nakagawa M, Koyanagi M, Tanabe K, *et al.* 2008; Generation of induced pluripotent stem cells without Myc from mouse and human fibroblasts. *Nat Biotechnol* **26:** 101–106.

Oda Y, Yoshimura Y, Ohnishi H, *et al.* 2010; Induction of pluripotent stem cells from human third molar mesenchymal stromal cells. *J Biol Chem* **285:** 29270–29278.

Ohgushi H, Caplan AI, 1999; Stem cell technology and bioceramics: from cell to gene engineering. *J Biomed Mater Res* **48:** 913–927.

Ohgushi H, Kotobuki N, Funaoka H, *et al.* 2005; Tissue engineered ceramic artificial joint – *ex vivo* osteogenic differentiation of patient mesenchymal cells on total ankle joints for treatment of osteoarthritis. *Biomaterials* **26:** 4654–4661.

Okita K, Ichisaka T, Yamanaka S, 2007; Generation of germline-competent induced pluripotent stem cells. *Nature* **448:** 313–317.

Patel M, Yang S, 2010; Advances in reprogramming somatic cells to induced pluripotent stem cells. *Stem Cell Rev* **6:** 367–380.

Salem HK, Thiemermann C, 2009; Mesenchymal stromal cells: current understanding and clinical status. *Stem Cells* **28:** 585–596.

Takahashi K, Tanabe K, Ohnuki M, *et al.* 2007; Induction of pluripotent stem cells from adult human fibroblasts by defined factors. *Cell* **131:** 861–872.

Takahashi K, Yamanaka S, 2006; Induction of pluripotent stem cells from mouse embryonic and adult fibroblast cultures by defined factors. *Cell* **126:** 663–676.

Vierbuchen T, Ostermeier A, Pang ZP, *et al.* 2010; Direct conversion of fibroblasts to functional neurons by defined factors. *Nature* **463:** 1035–1041.

Wernig M, Meissner A, Cassady JP, *et al.* 2008; c-Myc is dispensable for direct reprogramming of mouse fibroblasts. *Cell Stem Cell* **2:** 10–12.

Yoshimura K, Sato K, Aoi N, *et al.* 2008; Cell-assisted lipotransfer for cosmetic breast augmentation: supportive use of adipose-derived stem/stromal cells. *Aesthetic Plast Surg* **32:** 48–55, discussion 56–57.

Yu J, Vodyanik MA, Smuga-Otto K, *et al.* 2007; Induced pluripotent stem cell lines derived from human somatic cells. *Science* **318:** 1917–1920.

Zhou H, Wu S, Joo JY, *et al.* 2009; Generation of induced pluripotent stem cells using recombinant proteins. *Cell Stem Cell* **4:** 381–384.

# Simple Display System of Mechanical Properties of Cells and Their Dispersion

**Yuji Shimizu[1], Takanori Kihara[1]*, Seyed Mohammad Ali Haghparast[1], Shunsuke Yuba[2], Jun Miyake[1]**

**1** Department of Mechanical Science and Bioengineering, Graduate School of Engineering Science, Osaka University, Toyonaka, Osaka, Japan, **2** Health Research Institute, National Institute of Advanced Industrial Science and Technology (AIST), Amagasaki, Hyogo, Japan

## Abstract

The mechanical properties of cells are unique indicators of their states and functions. Though, it is difficult to recognize the degrees of mechanical properties, due to small size of the cell and broad distribution of the mechanical properties. Here, we developed a simple virtual reality system for presenting the mechanical properties of cells and their dispersion using a haptic device and a PC. This system simulates atomic force microscopy (AFM) nanoindentation experiments for floating cells in virtual environments. An operator can virtually position the AFM spherical probe over a round cell with the haptic handle on the PC monitor and feel the force interaction. The Young's modulus of mesenchymal stem cells and HEK293 cells in the floating state was measured by AFM. The distribution of the Young's modulus of these cells was broad, and the distribution complied with a log-normal pattern. To represent the mechanical properties together with the cell variance, we used log-normal distribution-dependent random number determined by the mode and variance values of the Young's modulus of these cells. The represented Young's modulus was determined for each touching event of the probe surface and the cell object, and the haptic device-generating force was calculated using a Hertz model corresponding to the indentation depth and the fixed Young's modulus value. Using this system, we can feel the mechanical properties and their dispersion in each cell type in real time. This system will help us not only recognize the degrees of mechanical properties of diverse cells but also share them with others.

**Citation:** Shimizu Y, Kihara T, Haghparast SMA, Yuba S, Miyake J (2012) Simple Display System of Mechanical Properties of Cells and Their Dispersion. PLoS ONE 7(3): e34305. doi:10.1371/journal.pone.0034305

**Editor:** Laurent Kreplak, Dalhousie University, Canada

**Received** December 23, 2011; **Accepted** February 25, 2012; **Published** March 30, 2012



**Funding:** This study was supported by grants from Okinawa Prefecture, Japan (http://www.pref.okinawa.jp/english/index.html) (research project of industrialization of medical innovation and technology to J.M.) and Graduate School of Engineering Science, Osaka University, Japan (http://www.es.osaka-u.ac.jp/eng/index.html) (Multidisciplinary Research Laboratory System to T.K.). The funders had no role in study design, data collection and analysis, decision to publish, or preparation of the manuscript.

**Competing Interests:** The authors have declared that no competing interests exist.

* E-mail: takanori.kihara@gmail.com

## Introduction

The primary method of material recognition by humans is visualization, and other available methods are contact force and tactile sense (i.e., haptics). In particular, in the recognition of material that is not directly visible, haptics provides unique information. Furthermore, haptics is the fundamental nature of material recognition in all forms of life. The information of the haptics of a given material is one of the important tools for communication and sharing the features of the material.

The mechanical properties of biological cells are unique indicators of their states. Malignant cancer cells exhibit lesser stiffness than normal cells [1]. Red blood cells infected with *Plasmodium falciparum* exhibit higher stiffness than uninfected cells [2]. In optic-cup morphogenesis, the stiffness alterations of the retinal epithelium are important for the self-formation of neural retina tissue [3]. Furthermore, the information of the stiffness of mesenchymal stem cells (MSCs) is related to their diverse characters and states [4–6]. The reasons for the importance of the mechanical properties of cells are that the mechanical properties are largely determined by the actin cytoskeleton [6–10]. The actin cytoskeleton is the essential element for regulating cell function [11–13].

Several techniques have been successfully employed to study the mechanical properties of cells, including micropipette aspiration, magnetic twisting cytometry, optical traps, and atomic force microscopy (AFM) [14–16]. The latter method can be used to image live cells and probe their mechanical properties in physiological conditions in a nondestructive manner and at a high spatial resolution [17,18]. It analyzes the mechanical properties of a living cell by the probe indentation method [7,19] and force modulation method [20]. In the probe indentation method, which is viscerally and easily comprehensible, an AFM cantilever serves as a microindenter to probe the cell directly.

Although the mechanical properties of a cell can be examined by using these methods, it is difficult to perceive the mechanical properties of cells and their cell type-specific differences, because the size of a cell is too small and the values of the mechanical properties of a cell exhibit very broad distributions, even for the same point on a cell [6]. It is also difficult to communicate or share the mechanical information of a cell with other people based on only numerical values. If the mechanical properties of a cell can be perceived via a system, then these issues can be resolved and many people will understand the mechanical information of a cell, thereby stimulating the research field of cell mechanics. Moreover, we can comprehend the mechanical interaction between 2 adjacent cells and between a cell and its physical microenvironment.